Pure & Appl.Chem., Vol.52, pp.2143-2160.
Pergamon Press Ltd. 1980. Printed in Great Britain.

Plenary Paper - Ion Exchange and Modification

ZEOLITE EXCHANGERS – SOME EQUILIBRIUM AND KINETIC ASPECTS

R.M. Barrer

Physical Chemistry Laboratories, Chemistry Department,
Imperial College, London SW7, UK

ABSTRACT

Cation exchange in zeolites has equilibrium and kinetic aspects. Equilibrium aspects considered were: evaluation of thermodynamic equilibrium constants from Kielland plots; the modifying role of intraphase exchange equilibria between sub-lattices on overall equilibrium constants and activity ratios; and a statistical thermodynamic treatment for a zeolite providing either a single cation sub-lattice or n sub-lattices. The statistical thermodynamic treatment includes replacements Na,Al $\rightleftarrows$ Si or Ca,Al $\rightleftarrows$ Na,Si. In the area of kinetics self-diffusivity was reviewed and some generalisations attempted.

INTRODUCTION

Cation exchange in zeolites is a readily controlled reaction, usually occurring easily below 100°C and involving simple isomorphous replacements of cations within aluminosilicates. Cation exchange also occurs with felspars and felspathoids, but at higher temperatures because the frameworks are less open and therefore the cations are less mobile. Like any other reaction ion exchange has equilibrium, kinetic and energetic aspects. This account will refer to features of the first two aspects.

EQUILIBRIUM

Isotherms have typical contours, several of which are shown in Fig. 1 [1,2,3,4]. Fig. 1d shows a miscibility gap, associated with hysteresis. Hysteresis characterises reversible solid state reactions in which a new phase nucleates on or in a matrix of a parent phase. It is ascribable to positive free energy terms associated with strain due to misfit of germ nuclei in the parent crystal and to interfacial free energy between nuclei and parent matrix. These terms on both forward and reverse reaction paths delay growth of the new phase beyond the true equilibrium between bulk A-rich phase and separate bulk B-rich phase, where A and B are the exchange cations. Within the hysteresis loop some remarkable history-dependent scanning curves and related

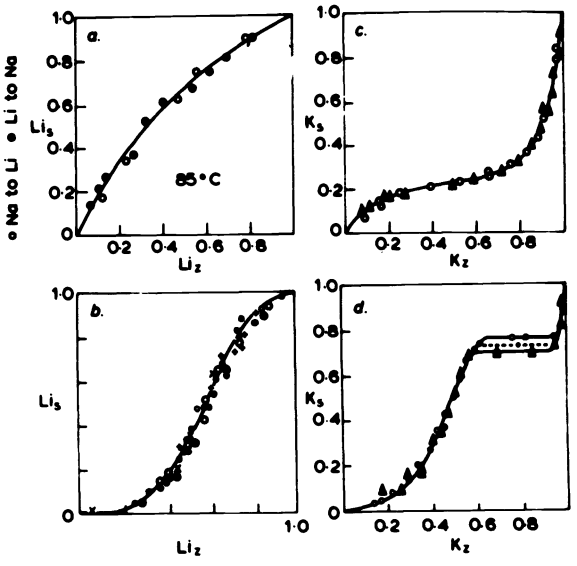

Fig. 1. Characteristic contours of exchange isotherms in some zeolites. Ordinate is equivalent cation fraction in solution; abscissa is this fraction in solution
(a) Li ⇄ Na in sodalite hydrate [2].
(b) Li ⇄ Na in cancrinite hydrate [2].
O, 25°C; o, 85°C; X 110°C for Na → Li
●, 25°C; ●, 85°C; +, 110°C for Li → Na
(c) Na ⇄ K at 25°C in Na-P [3].
O, K entering crystals;
▲, Na entering.
(d) Na ⇄ K at 25°C in K-F [4].
O, K entering crystals;
▲, Na entering

effects have been observed [2,5].

In many zeolites cations are distributed between various physically and crystallographically distinct site groups or sub-lattices (these terms are equivalent and will be used interchangeably). Equilibrium intraphase distributions of ions A and B are established between site groups, a property which has also been rather extensively studied in non-zeolites [7,8,9,10,11,12]. These include spinels (2 sub-lattices) and silicates (eqs. orthopyroxene with 2, garnets with 3 and cummingtonite with 4 sub-lattices). Zeolites are however unusual in that the total of cation sites can exceed the number of cations needed for electrical neutrality so that both cations and cation vacancies are distributed among the sub-lattices. I will return to this aspect after considering Kielland plots.

KIELLAND PLOTS

For the general exchange reaction

$$Z_A B_c^{Z_B} + Z_B A_s^{Z_A} \rightleftarrows Z_A B_s^{Z_B} + Z_B A_c^{Z_A}$$

Z_A and Z_B are the charges on the ions A and B and subscripts c and s denote in crystal and in solution respectively. Two important quotients are

$$K = \frac{(a_c^A)^{Z_B}(a_s^B)^{Z_A}}{(a_c^B)^{Z_A}(a_s^A)^{Z_B}}; \qquad K_c = \frac{A_Z^{Z_B}(a_s^B)^{Z_A}}{B_Z^{Z_A}(a_s^A)^{Z_B}} \qquad (1)$$

where the a denote activities and A_Z and B_Z are equivalent cation fractions of A and B in the zeolite. The ratio $(a_s^B)^{Z_A}/(a_s^A)^{Z_B}$ in solu-

tion can be measured. The thermodynamic equilibrium constant is obtained from plots of log K_c vs A_Z (Kielland plots). These are sometimes nearly linear but more often are not; they may have maxima or minima or both. Whatever their form log K_c may be represented as a polynomial in A_Z:

$$\log K_c = C_o + 2C_1 A_Z + 3C_2 A_Z^2 + ... \quad (2)$$

where the coefficients C are independent of A_Z. Gaines and Thomas [13] showed further that

$$\log E = \log (f_Z^A)^{Z_B}/(f_Z^B)^{Z_A} = 0.4343(Z_B-Z_A) - \log K_c + \int_o^1 \log K_c dA_Z + \Delta \quad (3)$$

where f_Z^A and f_Z^B are activity coefficients of A and B in association respectively with anionic framework elements L_A and L_B carrying Z_A and Z_B negative charges. Δ is a small term which is usually negligible for zeolites [14]. Eqns 1, 2 and 3 with $\Delta \sim 0$ lead to

$$\log E = 0.4343 (Z_B-Z_A) + C_1 (1-2A_Z) + C_2 (1-3A_Z^2) + ... \quad (4)$$

$$\log K = 0.4343 (Z_B-Z_A) + C_o + C_1 + C_2 + ... \quad (5)$$

For linear Kielland plots $\log K = 0.4343 (Z_B-Z_A) + C_o + C_1$ and if $Z_A = Z_B$ the first term on the r.h.s. of eqn 5 is zero. The standard free energy, $\Delta G^\ominus = - RT \ln K$ and the standard heat, $\Delta H^\ominus$, and entropy, $\Delta S^\ominus$, are obtained from $\Delta H^\ominus = - T^2 \partial(\Delta G^\ominus/T)/\partial T$ and $\Delta S^\ominus = - \partial \Delta G^\ominus/\partial T$. Accordingly Kielland plots can give useful thermodynamic information.

When the isotherm is strongly selective for one ion the curve of A_S vs A_Z is very close to the ordinate at one end and the abscissa at the other, and Kielland plots tend to become inaccurate at these extremities. This can introduce error in evaluating K from Kielland plots. A second factor often inadequately tested is isotherm reversibility. Points for forward and reverse exchanges should be shown to lie on the same curve.

CATION EXCHANGERS PROVIDING n SUB-LATTICES

We firstly note, as pointed out by Mueller et al. [10] that "chemical potentials of atoms or ions on non-equivalent lattice sites have no validity because these particles cannot be considered independently variable components". They also pointed out that this fact in no way prevents formulation of intraphase equilibrium constants and standard free energies of exchange of ions A and B between sub-lattices. Several procedures are possible, one of which, due to Mueller, [8] is based on detailed balancing, and is summarised below for a zeolite having n sub-lattices.

If the cations A and B have the same charge the rate of change of concentration of A on sub-lattice i is

$$\frac{dC_i^A}{dt} = \sum_{j=1}^{n-1} k'_{ji} (\phi_j^A C_j^A)(\phi_i^B C_i^B) - \sum_{j=1}^{n-1} k'_{ij} (\phi_i^A C_i^A)(\phi_j^B C_j^B) \quad (6)$$

The C are molar concentrations or number densities (per cm^3) of the cations indicated by the superscripts, on site groups indicated by the

subscripts. The k' are rate constants in concentration units. The ϕ may be regarded as the equivalent of activity coefficients in macroscopic systems and allow for deviations from ideal mixing of A and B on the sub-lattices. In energy terms they reflect any variability in the Gibbs free energy of intraphase exchange between sub-lattices other than that attributable to the entropy of mixing.

If A_i, B_i and A_j, B_j are equivalent cation fractions of ions A and B on site-groups i and j respectively, then eqn 6 can be re-written as

$$\frac{dA_i}{dt} = \sum_{j=1}^{n-1} k_{ji}(\phi^A_j A_j)(\phi^B_i B_i) - \sum_{j=1}^{n-1} k_{ij}(\phi^A_i A_i)(\phi^B_j B_j) \qquad (7)$$

where $k_{ji} = k'_{ji}(C^A_j + C^B_j)$ and $k_{ij} = k'_{ij}(C^A_j + C^B_j)$. At equilibrium, when $dA_j/dt = 0$, the pairs of terms in eqn 7 independently add to zero (principle of microscopic reversibility) and so

$$K_{ji} = \frac{k_{ji}}{k_{ij}} = \frac{(\phi^A_i A_i)(\phi^B_j B_j)}{(\phi^A_j A_j)(\phi^B_i B_i)} \qquad (8)$$

Eqn 8 can be re-written as

$$\frac{(\phi^A_i A_i)a^B_s}{(\phi^B_i B_i)a^A_s} \Big/ \frac{(\phi^A_j A_j)a^B_s}{(\phi^B_j B_j)a^A_s} = K_i/K_j = K_{ji} \qquad (9)$$

where K_i and K_j are equilibrium constants for exchange of A and B between ambient solution and sites on sub-lattices i and j respectively. a^A_s and a^B_s are the activities of A and B in solution at equilibrium. Eqn 9 thus leads to the general relation [15] for equilibria between solution and each of n site-groups (i.e. sub-lattices):

$$\frac{a^B_s}{a^A_s} = \frac{a^B_Z}{a^A_Z} K = \frac{a^B_1}{a^A_1} K_1 = \cdots = \frac{a^B_i}{a^A_i} K_i = \cdots = \frac{a^B_n}{a^A_n} K_n \qquad (10)$$

where

$$a^B_i/a^A_i = \phi^B_i B_i/\phi^A_i A_i \qquad (11)$$

Eqn 10 contains the overall equilibrium constant, K, and activity ratio a^B_Z/a^A_Z. If X_i is the fraction of total cationic charge associated with the i^{th} site group then eqn 10 gives

$$\frac{a^A_Z}{a^B_Z}(K_1^{X_1} \cdots K_n^{X_n}) = K\left[\left(\frac{a^A_1}{a^B_1}\right)^{X_1} \cdots \left(\frac{a^A_n}{a^B_n}\right)^{X_n}\right] \qquad (12)$$

Also the overall standard free energy of exchange is the sum of the corresponding exchange reactions on all the sub-lattices and so

$$\Delta G^{\Theta} = \sum_{i=1}^{n} X_i \Delta G^{\Theta}_i \qquad (13)$$

Thus with $\Delta G^{\ominus} = - RT \ln K$ and $\Delta G_i^{\ominus} = - RT \ln K_i$, eqns 12 and 13 give

$$\left.\begin{aligned} K &= K_1^{X_1} \ldots\ldots K_n^{X_n} \\ \frac{a_Z^A}{a_Z^B} &= \left(\frac{a_1^A}{a_1^B}\right)^{X_1} \ldots\ldots \left(\frac{a_n^A}{a_n^B}\right)^{X_n} \end{aligned}\right\} \qquad (14)$$

Eqns 14 show how equilibria on sub-lattices influence the overall equilibrium constant and activity ratio. Some general consequences are [16]:

(i) When for simplicity we take n = 2 with ideal exchange on each site group (Ø's all unity), and if $K_1 > 1$ and $K_2 < 1$, then the resultant isotherm of A_s vs A_Z is sigmoid in form even where $K = K_1^{X_1} K_2^{X_2} = 1$. For n = 1 and K = 1 an ideal isotherm would be a straight line of unit slope. Thus the mixture of two ideal component isotherms is non-ideal as regards the overall isotherm.

(ii) Ideal component isotherms can never give miscibility gaps in the overall isotherm.

(iii) Without additional information a given overall isotherm cannot be analysed to give component isotherms because numerous empirical allocations of the K_i and X_i (i = 1 to n) of the first of eqns 14 could give the correct K.

Much additional information comes, however, from X-ray structural evidence. This gives the number, n, of sub-lattices and the values of $X_1, X_2 \ldots$. If X-ray or other means could further give the cation fraction of each ion actually present on each sub-lattice as a function of cation composition then Kielland plots for each sub-lattice would give the K_i and the ratio $Ø_i^A/Ø_i^B$. Two numerical examples of applications of eqns 14 follow.

(a) In zeolite K-F, $Na^+ \rightleftarrows Li^+$, $Na^+ \rightleftarrows K^+$ and $Na^+ \rightleftarrows Cs^+$ were studied [4]. Two site groups were assumed and from the sigmoid $Na^+ \rightleftarrows Cs^+$ isotherm (Fig. 2) $X_1/X_2 = 0.64/0.36$ was found. Subsequent X-ray studies [17] showed K-F in its Na-, K- and Rb-forms to be of edingtonite type with two kinds of channel each bearing cations. Experimental isotherms

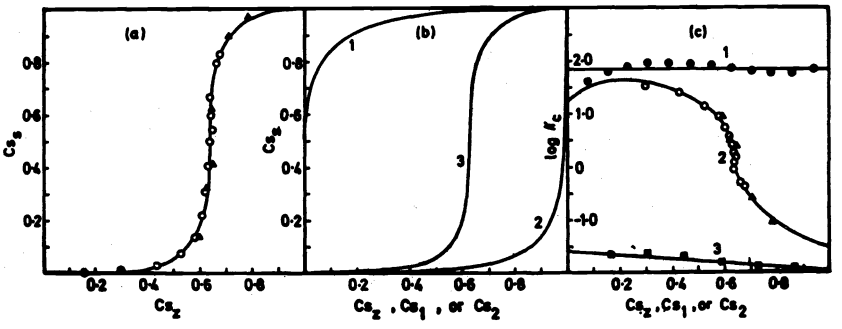

Fig. 2. (a) The Na ⇄ Cs isotherm in K-F [4]. O, Cs entering crystals; Δ, Na entering.
(b) Analysis of isotherm in terms of two site groups. Curve 1, isotherm on sites of first kind; curve 2, isotherm on sites of second kind; curve 3, resultant isotherm.
(c) The assumed Kielland plots on sites of first kind (curve 1), second kind (curve 3) and resultant isotherm (curve 2).

were successfully reproduced assuming linear Kielland plots with assigned coefficients C_{11} and C_{12} for each site group, and values of K_1 and K_2. Results are exemplified in Fig.2 for $Na^+ \rightleftarrows Cs^+$, while the assigned values for the other two exchanges are given below:

Exchange	C_{11}	C_{12}	K_1	K_2
$Na^+ \rightleftarrows K^+$	- 0.33	1.55	4.57	0.374
$Na^+ \rightleftarrows Li^+$	0	1.27	1.11	0.89

(b) (Fe,Mg)-olivine (one site group) and (Fe,Mg)-orthopyroxene (two site groups) are found as co-existing phases, and the $Fe^{2+} \rightleftarrows Mg^{2+}$ distributions between the two phases and between the two sub-lattices of orthopyroxene have been studied [11,18]. The olivine with one site group plays the role of the aqueous medium. At 900°C $\Delta G^{\theta} \simeq$ - 7.3 kJ mol^{-1} for $Fe^{2+} \rightleftarrows Mg^{2+}$ between the phases and $\Delta G^{\theta}_{12} \simeq$ -12.3 kJ mol^{-1} for $Fe^{2+} \rightleftarrows Mg^{2+}$ between the two sub-lattices of orthopyroxene.

STATISTICAL THERMODYNAMIC DEVELOPMENTS

An adequate theoretical treatment must explain and be able to represent the contours of different isotherm types (Fig. 1) and of Kielland plots, and also the existence and extent of miscibility gaps. Progress has been made with the following model and its statistical thermodynamic formulation [2,19,20].

Miscibility gaps are manifestations of a tendency sometimes shown for ions of a given kind to cluster and so to nucleate a new phase. The simplest assumption which accounts for this is that if for example two ions A occupied adjacent sites an extra relaxation of the framework and/or cation shift occurs which does not happen when A or B is adjacent to B or to a vacant site [2,19]. The extra energy change associated with this relaxation is conveniently written as $2w_{AA}/\nu$ where ν is the co-ordination number of a site. It is assumed to be pairwise additive. In systems where n = 1 (one site group only) and where vacancies may occur the above model has been extended to pairwise-additive extra relaxation energies $2w_{AA}/\nu$, $2w_{BB}/\nu$ and $2w_{AB}/\nu$ for AA, BB and AB pairings, as compared with OO, OA and OB where O denotes a vacant site [20] These energies, though referred to cation pairings, are thought to be very much functions of misfit in the anionic frameworks which cause local adjustments.

The model described has been developed for exchangers with a single cation sub-lattice, for ideal exchange on n sub-lattices, and for exchanges involving replacement of Si by Al (e.g. Na,Al $\rightleftarrows$ Si; Ca,Al $\rightleftarrows$ Na,Si).

Single Site Group When, as in sodalite hydrate, only one kind of exchange site is involved and $2w_{AA}/\nu$ is the only extra relaxation energy, the partition function, P, for the mixed crystal takes the form

$$P = \frac{N!}{N_A!N_B!(N-N_A-N_B)!} J_A^{N_A} J_B^{N_B} J_G^{N_G} P_L^{N_O} P_{int} \qquad (15)$$

where N = total number of sites; N_A and N_B are the numbers of ions of A and B and N_G of guest molecules (water); J_A, J_B and J_G are partition functions for individual cations A and B and for a guest molecule. $J_G^{N_G} = C(N_G)(J_G)^{N_G}$ and contains a configurational part $C(N_G)$, but for simplicity N_G is assumed not to change as a result of exchange so that $C(N_G)$ is a constant and need not be evaluated for present purposes.

The partition function for that amount of framework carrying one negative charge is P_L and the total anionic charge is $N_o = Z_A N_A + Z_B N_B$. P_L is assumed constant, and the extra relaxation energy $2w_{AA}/\nu$ introduces the contribution P_{int} to the overall partition function, P. With J_A, J_B, J_G and P_L independent of composition of the (A,B)-zeolite interest centres on the factorial quotient and P_{int}. The Helmholtz free energy is $F = -kT \ln P$. The contribution to F from P_{int} was shown to be

$$F_{int} = kT\,\nu \left\{ N_A \ln \frac{2(1-\theta_A)}{D_{AA}-2\theta_A} + \frac{N}{2} \ln \frac{D_{AA}-2\theta_A}{D_{AA}(1-2\theta_A)} \right\} \qquad (16)$$

where

$$\left.\begin{aligned} D_{AA} &= \left[1 - 4\theta_A(1-\theta_A)\alpha_{AA}\right]^{\frac{1}{2}} + 1 \\ \alpha_{AA} &= 1 - \exp - 2w_{AA}/\nu kT \\ \theta_A &= N_A/N \end{aligned}\right\} \qquad (17)$$

Expressions were obtained for the chemical potentials μ_{AL_A} and μ_{BL_B} for the components of the zeolite considered as a two component system comprising N_A units of AL_A plus guest molecules as the first and N_B units of BL_B with guest molecules as the second. As assumed above the number of guest molecules per unit is the same for each component. L_A and L_B are the amounts of anionic framework carrying Z_A and Z_B negative charges and associated respectively with cations A and B carrying Z_A and Z_B positive charges. From the standard chemical potentials the equilibrium constants were obtained for $Z_A Z_B$ equivalents of exchange as

$$RT \ln K = Z_A \mu^{\ominus}_{BL_B} - Z_B \mu^{\ominus}_{AL_A} + Z_B \mu^{\ominus}_{A_s} - Z_A \mu^{\ominus}_{B_s} \qquad (18)$$

and also explicit expressions were found for the activity coefficients. When $Z_A = Z_B$ these reduce to

$$\ln f_A/f_B = (\Delta_A - \Delta_A^*)/\Delta_B \qquad (19)$$

where

$$\Delta_A = \frac{1}{kT}\left(\frac{\partial F_{int}}{\partial N_A}\right)_{BL_B} ; \quad \Delta_B = \frac{1}{kT}\left(\frac{\partial F_{int}}{\partial N_B}\right)_{AL_A} \qquad (20)$$

and Δ_A^* is the value of Δ_A in the standard state. For AL_A and BL_B the standard states were homoionic A- and homoionic B-zeolite respectively. Thus by allocating values of $2w_{AA}/\nu$, ν and N the isotherms could be calculated. They represented all the types shown in Fig.1, including isotherms with miscibility gaps for sufficiently large exothermal values of $2w_{AA}/\nu$ [19,20].

It is of interest that strictly linear Kielland plots are not expected when F_{int} is given by eqn 16. Linear plots require that despite non-zero values of $2w_{AA}/\nu$, the cations should be randomly distributed on the sites. True randomness is not however compatible with non-zero $2w_{AA}/\nu$. In the limiting case of linear Kielland plots C_1 in eqn 2 is given by [2]

$$2.303\, C_1 = \frac{-w_{AA}(N_A + N_B)}{N\,kT} \qquad (21)$$

Table 1

Coefficients C_1 and values of $w_{AA}(N_A + N_B)/N$ [1]

Exchanger	Exchange	T°C	C_1	$w_{AA}(N_A + N_B)/N$ (kJ/g ion)
Chabazite	Na → Rb	84	- 1.0	6.8
	Na → Tl	45	- 0.30	1.8_4
	Na → Ag	45	0	0
	K → Ag	25	- 0.44	2.5_1
Cancrinite	Li → Na	~68	- 1.08	7.1
Faujasite	Na → Ag	25	- 0.48	2.7_6
	K → Ag	25	- 0.49	2.8_1
	Na → K	25	- 0.52	2.9_8
	Tl → Ag	25	- 0.68	3.8_9

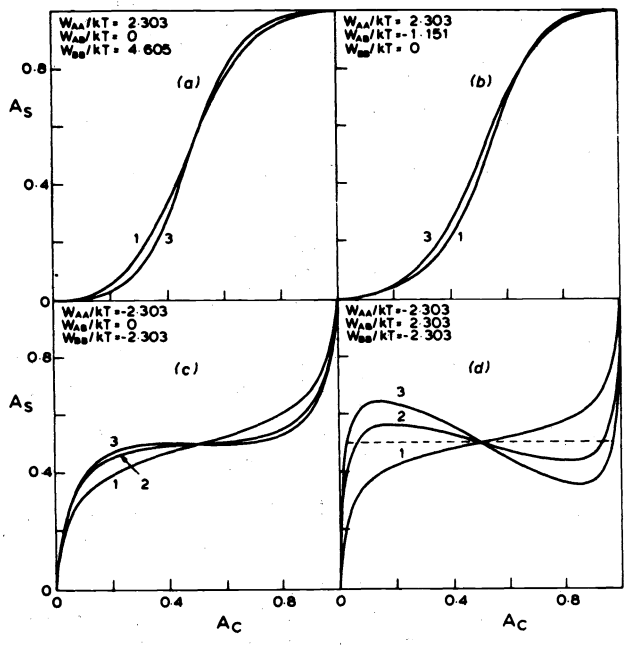

Fig. 3. Exchange isotherms for $Z_A = Z_B = 1$, $K = 1$, and $\eta = N/(Z_A N_A + Z_B N_B) = 2$. For curves 1 $\nu = 2$, for curves 2 $\nu = 4$ and for curves 3 $\nu = 6$. In (a) $\Sigma = (w_{AA} - 2w_{AB} + w_{BB})/kT = 6.908$, in (b) $\Sigma = 4.605$, in (c) $\Sigma = -4.605$ and in (d) $\Sigma = -9.210$. All isotherms were calculated assuming $\mu^{\theta}_{A_s} - \mu^{\theta}_{B_s} = 0$. Miscibility gaps in (d) are indicated by dashed line [20].

and in several systems where the experimental Kielland plots were approximately linear the coefficients C_1 and values of $w_{AA}(N_A + N_B)/N$ are presented in Table 1 [1].

For the more complex situation where extra energies $2w_{AA}/\nu$, $2w_{BB}/\nu$ and $2w_{AB}/\nu$ were involved order-disorder theory [21,22] was used [20]. Again for a single site group all the isotherm types of Fig.1 could be reproduced and for adequately exothermal $2w_{AA}/\nu$ or $2w_{BB}/\nu$ miscibility gaps again appeared (Fig.3). Endothermal $2w_{AB}/\nu$ had a similar effect to exothermal $2w_{AA}/\nu$ or $2w_{BB}/\nu$ in causing like ions to cluster. This tendency was a function of $\Sigma = (w_{AA} - 2w_{AB} + w_{BB})/kT$.

Exchanger with n Site Groups. The partition function now takes the form

$$P = \prod_{i=1}^{n} P_i = \prod_{i=1}^{n} \frac{N_i!}{N_{A,i}!N_{B,i}!(N_i - N_{A,i} - N_{B,i})!} J_{A,i}^{N_{A,i}} J_{B,i}^{N_{B,i}} J_{G,i}^{N_{G,i}} P_{L,i}^{N_{o,i}} \qquad (22)$$

where the P_i for the ions A and B on the i^{th} sub-lattice (i=1 to n) has the same form as eqn 15, but P_{int} is for simplicity taken as unity for each sub-lattice (i.e. the ideal case is assumed with the $\emptyset$ of eqn 11 all unity and so $K_{c,i} = K_i$). From eqn 22 the Helmholtz free energy in the mixed crystal and in the standard states (pure AL_A and BL_B respectively) were obtained, and hence the overall equilibrium constant. The contributions to $F^{\ominus}_{AL_A}$ and $F^{\ominus}_{BL_B}$ from the i^{th} sub-lattice were all identifiable and are termed $\left(F^{\ominus}_{AL_A}\right)_i$ and $\left(F^{\ominus}_{BL_B}\right)_i$ per molar unit $(AL_A)_i$ and $(BL_B)_i$. From the expressions for $F^{\ominus}_{AL_A}$ and $F^{\ominus}_{BL_B}$ per mole of AL_A and BL_B one finds

$$F^{\ominus}_{AL_A} = \sum_{i=1}^{n} X_i \left(F^{\ominus}_{AL_A/i}\right) \quad ; \quad F^{\ominus}_{BL_B} = \sum_{i=1}^{n} X_i \left(F^{\ominus}_{BL_B}\right)_i \qquad (23)$$

The equilibrium constant, K_i, between ions in solution and ions on the i^{th} sub-lattice for $Z_A Z_B$ equivalents of exchange, is then

$$RT \ln K_i = Z_A \left(F^{\ominus}_{BL_B}\right)_i - Z_B \left(F^{\ominus}_{AL_A}\right)_i + Z_B \mu^{\ominus}_{A_s} - Z_A \mu^{\ominus}_{B_s} \qquad (24)$$

Eqns 18, 23 and 24 together recover the first of eqns 14 ($K = K_1^{X_1} \ldots\ldots K_n^{X_n}$).

Particular situations examined included n=2, with one site group available to A and B and the second only to B. Isotherms taking K=1 (unprimed numbers on curves) and K=10 (primed numbers) are shown in Fig. 4. For curves 1 and 1', 2 and 2', 3 and 3', 4 and 4' and 5 and 5' the maximum exchanges of B by A were respectively $A_Z^{max} = 0.6$, 0.7, 0.8, 0.9 and 1.0. Isotherms 1' and 2' have contours resembling those obtained when transition metal ammine ions (ions A) exchange with NH_4^+ (ions B) in mordenite, [23] except that A_Z^{max} was ~ 0.5. The metal ammine ions are thought to be too bulky to enter the side pockets lining the wide channels in mordenite, but NH_4^+ should do so. The evidence is then that at the limit of exchange ~ 50% of NH_4^+ still remains in side pockets.

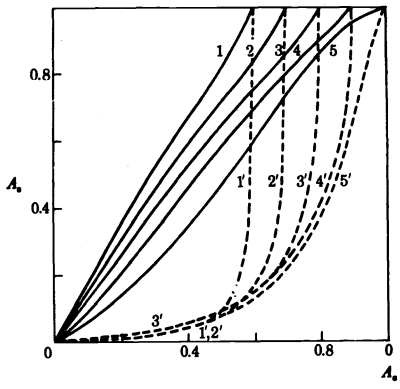

Fig. 4. Exchange isotherms calculated for zeolite with two site groups, 1 and 2 [19]. 1 is available to univalent ions A and B; 2 is available only to B. Isotherms with solid lines have K = 1; and with dashed lines K = 10. $N/(N_A + N_B) = 1$. For values of A_c^{max} see text.

Isomorphous Replacements involving Al and Si. So far ion exchanges within a framework of fixed composition w.r.t. Al and Si have been considered. The model and its treatment are however readily extended to include replacements such as Na,Al ⇄ Si and Ca,Al ⇄ Na,Si. [19] This requires consideration of the partition function for the aluminosilicate framework, P_L^{No} in eqns 15 or 22, because the framework composition is now changing. For simplicity all tetrahedral positions were regarded as equivalent, although this is not strictly true. When a tetrahedral unit AlO_4 replaces SiO_4 the energy of replacement was taken as ϵ_{Al}. When two AlO_4 replace two adjacent SiO_4 an extra pairwise-additive relaxation energy was assumed to arise. It was $2w/\nu = w/2$ since for tetrahedral sites the co-ordination number, ν, is 4. This extra energy, from Lowenstein's rule [24], is expected to be endothermic. The framework partition function of eqns 15 or 22 since there are no unoccupied tetrahedral sites, takes the form

$$P_L^{N_o} = \frac{N_\gamma!}{N_{Al}!N_{Si}!} \cdot J_{Si}^{N_{Si}} J_{Al}^{N_{Al}} P_{Al}^{int} \qquad (25)$$

N_γ is the total number of tetrahedral sites and N_{Al} and N_{Si} the numbers of AlO_4 and SiO_4 tetrahedra on these sites ($N_\gamma = N_{Al} + N_{Si}$). J_{Si} and J_{Al} are partition functions of an SiO_4 and an AlO_4 respectively and P_{Al}^{int} is the contribution to $P_L^{N_o}$ and so to the overall partition function, P, arising from the extra relaxation energy w/2. For F_{Al}^{int} corresponding with P_{Al}^{int} it was shown that

$$\left.\begin{aligned} F_{Al}^{int} &= 2kT\left\{2N_{Al}\ \ln\frac{2X_{Si}}{D-2X_{Al}} + N_\gamma\ \ln\frac{(D-2X_{Al})}{X_{Si}D}\right\} \\ D &= \left\{1 - 4X_{Al}X_{Si}\alpha\right\}^{\frac{1}{2}} + 1 \\ \alpha &= 1 - \exp - w/2kT \end{aligned}\right\} \qquad (26)$$

with $F = -kT \ln P$ as before, the free energy function $f(F) = F/kTN_\gamma + t_2$

was found and plotted against $X_{Al} = N_{Al}/N_\gamma$ for various values of adjustable parameters. The term t_2 is

$$t_2 = \ln \left[J_{Si} \, J_G^{N_G/N_\gamma} \right] \qquad (27)$$

where $J_G^{N_G}$ is the same as in eqns 15 and 22. Since N_G was assumed constant t_2 was also taken as a constant.

The function f(F) contains a linear term $X_{Al} t_1$ where

$$t_1 = \ln \left[J_{Si}/J_{Al} J_A^{1/Z_A} \right] \qquad (28)$$

for the homoionic A-zeolite. If the cations A behave as 3-dimensional harmonic oscillators and $J_{Si}/J_{Al} = \exp - \epsilon_{Al}/kT$ then for $\omega = 10^{13} s^{-1}$, T = 300K:

$$t_1 = \frac{1.7265}{Z_A} - 0.401 \left(\frac{\epsilon_A}{Z_A} + \epsilon_{Al} \right)$$

where ϵ_A is the binding energy of A and ϵ_{Al} the energy of replacement of SiO_4 by AlO_4. t_1 is + ve if $\epsilon_A + Z_A \epsilon_{Al} < 4.306$ kJ mol^{-1} and - ve for the reverse inequality. Plots of f(F) vs X_{Al} had the following properties:

(i) f(F) tends to have a minimum the position and depth of which depends on the magnitude and sign of t_1 and the magnitude of w/kT, both taken as adjustable parameters, except that w/kT > 0. For w/kT = 10 and t_1 = - 5 and - 10 the minima move nearer to X_{Al} = 0.5 as t_1 becomes more negative (Fig. 5a). When t_1 = - 15 and w/kT = 40 the curves are V-shaped with deep minima virtually at X_{Al} = 0.5. Therefore Al/Si ~ 1.0 and is fixed as found in the felspathoids nepheline, kalsilite and kaliophilite. (Fig. 5b)

(ii) When t_1 is positive and increasing, with w/kT = 40, the minima become shallow and move towards X_{Al} = 0 (Fig. 5c). Thus

t_1	= 2	4	6	8	10
X_{Al}^{min}	= 0.18	0.10	0.043	0.017	0.0065
Si/Al	= 4.56	9.0	22.3	57.8	152.8

Accordingly a possible criterion for formation of silica-rich zeolites such as ZSM-5 and ZSM-11 is a topology giving a large positive value of t_1.

(iii) When for the cation $w_{AA}/kT = 0$ the shape of the plot of f(F) vs X_{Al} depends only slightly upon the cation charge Z_A (curves 1 and 2 in Fig. 5b).

(iv) When there are enough or more than enough cation sites to reach a theoretical Al end member (X_{Al} = 1), then $N/N_\gamma = r_c$ influences the minimum more than the shape of the curve of f(F) vs X_{Al} (curves 1 and 3 of Fig. 5b). This influence operates through a term $r_c \ln r_c$ in f(F).

(v) A limit to isomorphous replacement in the framework is the smaller of $X_{Al}^{max} = 0.5$ (Lowenstein's rule, [24] exemplified in Fig. 5b) or $X_{Al}^{max} = Z_A r_c$. When $Z_A r_c < 0.5$ only part of the curve f(F) vs X_{Al} is realisable as shown in Fig. 6a for t_1 = - 15 and r_c = 1/6 (curve 1), 1/4 (curve 2) and 1/2 (curve 3), taking Z_A = 1. The tectosilicates then tend to have fixed compositions corresponding with the lowest realisable points on plots of f(F) vs X_{Al}.

(vi) When t_1 has small + ve or - ve values, with $w_{AA}/kT = 0$ for the cation and w/kT = 40, rather flat curves of f(F) vs X_{Al} are obtained

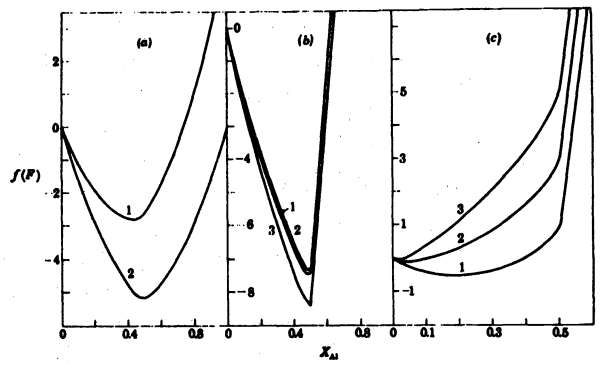

Fig. 5. Plots of f(F) against X_{Al} for $w_{AA}/kT = 0$. (a) $Z_A = 1$; $r_c = N/N_\gamma = 1$; $w/kT = 10$. For curve 1, $t_1 = -5$ and for curve 2 $t_1 = -10$. (b) $t_1 = -15$; $w/kT = 40$; for curve 1 $Z_A = 1$ and $r_c = 1$; for curve 2 $Z_A = 2$, $r_c = 1$; and for curve 3 $Z_A = 1$ and $r_c = 5$. (c) $Z_A = 1$; $r_c = 1$; $w/kT = 40$. For curve 1, $t_1 = 2$; for curve 2, $t_1 = 6$; and for curve 3, $t_1 = 10$.

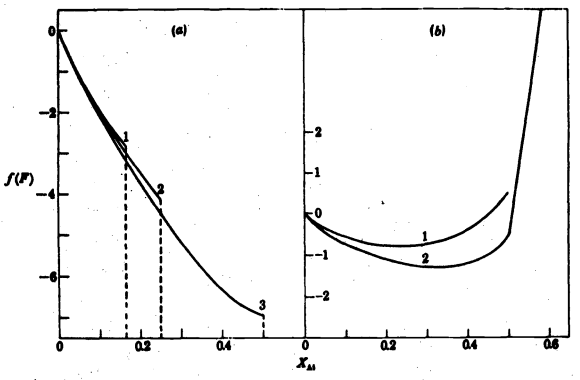

Fig. 6. Plots of f(F) against X_{Al} drawn for $Z_A = 1$, $w_{AA}/kT = 0$ and $w/kT = 40$ [19]. (a) $t_1 = -15$. For curve 1, $r_c = 1/6$; for curve 2, $r_c = 1/4$ and for curve 3, $r_c = 1/2$. (b) For curve 1, $t_1 = -0.2$ and $r_c = 1/2$; for curve 2, $t_1 = -1.1$ and $r_c = 1$.

with shallow minima (Figs. 5c and 6b). This suggests that such tectosilicates could, by varying the conditions of synthesis, be prepared with a range of values of Si/Al (e.g. chabazite, faujasite, zeolite L).

From the foregoing short account the statistical thermodynamic treatment, with the relatively simple model suggested, is seen able to present a very encouraging range of the properties observed in isomorphous replacement.

SELF-DIFFUSIVITIES OF IONS IN ZEOLITES

The expressions for ionexchange equilibria of ions A and B between sub-lattices were developed assuming ready mobility of cations. Self-diffusivities of cations have been measured in analcime, [25], chabazite, [26,27], zeolite A, [28,29,30,31,32], mordenite [33], and zeolites X and Y [28,29,32,34,35,36]. Results are summarised in Tables 2, 3 and 4. For most of the diffusivities, D*, which obey the relation $D^* = D_o \exp -E/RT$ (Fig. 7 [32]) the activation energies, E, are so large as to indicate that intracrystalline diffusion is the rate-controlling step. For boundary-layer control in the aqueous solution E would be ~ 16 kJ mol^{-1}.

In interpreting rates of exchange between traced and untraced ions in crystal and solution the surface area is involved. Two values have been used: smoothed or geometrical areas, G, based on crystal dimensions, or determined by flow methods; and BET areas, A, found by krypton adsorption (or an equivalent sorbate), under conditions where intracrystalline penetration does not occur. It is not clear which of

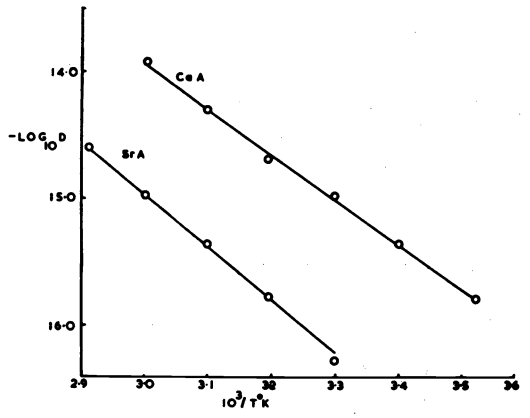

Fig. 7. Temperature dependence of D* ($cm^2 s^{-1}$) for Ca and Sr in zeolite A [32].

these areas is most appropriate and unfortunately the adsorption areas, A, can greatly exceed the geometrical areas, G. D* varies as $(\text{area})^{-2}$ and the differences between A and G can represent a factor as large as 10^3 in D*. Since the entropy of activation, ΔS^+, is derived from D_o (in $D^* = D_o \exp - E/RT$) using the relation

$$D_o = 2.72 \frac{kT}{h} d^2 \exp \Delta S^+/R \qquad (30)$$

and since the whole uncertainty in the area to be used is reflected in D_o, an uncertainty of 10^3 represents ~ 58 J K^{-1} mol^{-1} in ΔS^+. This uncertainty is related to estimates of ΔG^+, the free energy of activation :

$$\Delta G^+ = \Delta H^+ - T\Delta S^+ = E - RT - T\Delta S^+ \qquad (31)$$

In these relations k and h are Boltzmann's and Planck's constants and d is the jump distance per unit diffusion process. ΔH^+ is the heat of activation.

Despite the above uncertainty, and in addition the restricted ranges in temperature often involved (Tables 2 to 4), comparison of the results indicates the following behaviour:

(i) D_o tends in a given zeolite to increase as E increases. This is one more instance of the much more precise correlations observed between log D_o and E/T for diffusion in elastomers [40]. These correlations signify that in $\Delta G^+ = \Delta H^+ - T\Delta S^+$ where

$$\Delta G^+/RT = - \ln D^* + \ln [kTd^2/h] \qquad (32)$$

the experimentally accessible ranges in ln D* and hence in ΔG^+ are less than those in ΔH^+ and $T\Delta S^+$.

(ii) In the most compact zeolite, analcime, all forms studied were anhydrous except the Na-form. In analcime E increased with ion radius or polarisability of the monovalent cations [25]. In anhydrous zeolite X E for electrical conductivity also increased with ion radius for Ca^{2+}, Sr^{2+} and Ba^{2+} [39].

(iii) When the zeolites are hydrous (A, X, Y, chabazite, mordenite) E is not clearly related to crystallographic radii. Thus E is often less for Ba^{2+} than for Sr^{2+}. This suggests that energy barriers are influenced by the hydration shell. In anhydrous alcohol-anhydrous zeolite exchanges involving X and Y and ions Ca^{2+}, Sr^{2+} and Ba^{2+}, E is again a maximum for Sr^{2+}. With ethanol as solvent exchange proceeded more slowly than with methanol [35].

(iv) Cation charge is also important, as indicated by higher E in chabazite [26] for Ca^{2+}, Sr^{2+} and Ba^{2+} than for Na^+, K^+, Rb^+ and Cs^+.

Table 2 Self-diffusivities in A, X and Y ($D^* = D_o \exp -E/RT$; $k_2 = k_o \exp -E_1/RT$)

Zeolite	Composition	$D_o/m^2 s^{-1}$ (k_o/s^{-1})	$E/kJ\ mol^{-1}$ ($E_1/kJ\ mol^{-1}$)	Surface Area used and comments	Reference
Na-A	$Na_{12}[Al_{12}Si_{12}]$	$10^{-7.2 \pm 0.5}$ ($10^{5.7 \pm 0.6}$)	22.4 ± 3.0 (42.4 ± 3.3)	G; 3.4 - 38.5°C	28,29
Ca-A	~ 90% exchanged	$4.7_5 \times 10^{-8}$	67.3 ± 0.8	G; 10 - 60°C	32
Sr-A	~ 90% exchanged	7.4×10^{-8}	81.8 ± 0.8	G; 30 - 70°C	
Ba-A	"Ba-saturated"	1×10^{-5}	73.6	G; 45 - 141°C	30
Zn-A	$Zn_{5.5}Na_{0.9}[Al_{12}Si_{12}]$	$10^{-3.97 \pm 0.03}$ ($10^{3.05 \pm 0.25}$)	67.1 ± 0.5 (56.5 ± 1.5)	G; 25 - 60°C	31
Na-X	-	$10^{-4.1 \pm 0.21}$ ($10^{2.65 \pm 0.98}$)	40.5 ± 0.12 (19.7 ± 5.4)	G; 1.6 - 30°C	28,29
Ca-X	~ 90% exchanged	$1.4_5 \times 10^{-6}$	83.2 ± 1.3	G; -36 to -18°C; 50% C_2H_5OH - water mixture	32
Sr-X	~ 90% exchanged	$1.7_3 \times 10^{-2}$	83.6 ± 1.3	G; -30 to 0°C; 50% C_2H_5OH - water mixture	32
Ba-X	> 75% exchanged	$1.9_8 \times 10^{-2}$	84.0 ± 1.3	G; -24 to 0°C; 50% C_2H_5OH - water mixture	32
Sr-X	Near homoionic Al:Si=85:107	8×10^{-3}	127	G; 112 - 142°C	34
Ba-X	Near homoionic Al:Si=85:107	5×10^{-1}	66	G; 38 - 89°C	34
Sr-X	Near homoionic	1×10^{-7} (fast) 3×10^{-5} (slow)	36.8 (fast) 79.9 (slow)	G; 21 - 120°C	36
Ba-X	Near homoionic	2×10^{-8} (fast) 4×10^{-4} (slow)	40.6 (fast) 88.2 (slow)	G; 21 - 120°C	36
Ni-X	$Na_{5.5}Ni_{39.9}[Al_{85}Si_{107}]$	4.7×10^{-6}	86 ± 4	G; 75 - 140°C	37
Co-X	$Na_{7.4}Co_{38.8}[Al_{85}Si_{107}]$	9.1×10^{-6}	89 ± 4	G; 75 - 140°C	37
Ce-X	$Na_{8.6}Ce_{25.5}[Al_{85}Si_{107}]$	-	116 ± 6	G; -28 to -5°C; " "	38
Ni-Y	$Na_{1.8}Ni_{32.6}[Al_{67}Si_{125}]$	1.1×10^{-5}	100 ± 5	G; 75 - 140°C	37
Co-Y	$Na_{4.0}Co_{31.5}[Al_{67}Si_{125}]$	3.0×10^{-7}	90 ± 5	G; 75 - 140°C	37
Ce-Y	$Na_{7.2}Ce_{18.9}[Al_{67}Si_{125}]$	-	109 ± 5	G; -28 to -5°C; " "	38
Ni-Y	$Na_{2.2}Ni_{25.4}[Al_{53}Si_{139}]$	2.9×10^{-5}	107 ± 5	G; 75 - 140°C	37
Co-Y	$Na_{5.2}Co_{23.9}[Al_{53}Si_{139}]$	4.0×10^{-7}	90 ± 5	G; 75 - 140°C	37
Ce-Y	$Na_{4.5}Ce_{16.0}[Al_{53}Si_{139}]$	-	110 ± 6	G; -28 to -5°C; " "	38

Table 3. (a) Self diffusivities in zeolites X and Y in absence of water ($D^* = D_o \exp -E/RT$)

Zeolite	Composition	Solvent (M= methanol; E= ethanol)	$D_o/m^2 s^{-1}$	E/kJ mol^{-1}	Surface area used and comments	Reference
Ca-X	Near-homoionic Al:Si = 85:107	M	$2.5_9 \times 10^{-2}$	122	G; 34.4 - 61.3°C	35
Sr-X	"	M	v. slow			
Ba-X	"	M	$1.7_9 \times 10^{-3}$	103	G; 34.2 - 60.8°C	
Ca-,Sr- and Ba-X	"	E	v. slow			
Ca-Y	Near-homoionic Al:Si = 67:125	M	$1.8_7 \times 10^{-3}$	90.4	G; 29.4 - 59.3°C	
Sr-Y	"	M	$4.9_8 \times 10^{-5}$	118	G; 31.7 - 55.5°C	
Ba-Y	"	M	$6.4_7 \times 10^{-7}$	84.1	G; 45.6 - 62.3°C	
Ca-,Sr-Y	"	E	v. slow			
Ba-Y	"	E	$2.4_3 \times 10^{-4}$	120	G; 49.2 - 69.9°C	
Ca-Y	Near-homoionic Al:Si = 53:139	M	$9.3_3 \times 10^{-11}$	49.8	G; 20.0 - 38.1°C	
Sr-Y	"	M	$4.6_8 \times 10^{-6}$	91.6	G; 29.7 - 60.8°C	
Ba-Y	"	M	$2.1_2 \times 10^{-8}$	67.8	G; 28.7 - 49.1°C	
Ca-Y	"	E	$2.9_8 \times 10^{-13}$	58.2	G; 28.5 - 67.2°C	
Sr-Y	"	E	$4.1_9 \times 10^{-8}$	105	G; 51.8 - 76.9°C	
Ba-Y	"	E	$2.9_3 \times 10^{-8}$	91.6	G; 39.2 - 70.1°C	

(b) Electrical conductivity in anhydrous forms of zeolite X ($\sigma = \sigma_o \exp -E/RT$)

Ca-X	Near homoionic	None	-	87.4	Compacted plugs used; temperature range covered was between 226 and 727°C.	39
Sr-X	"	"	-	91.2		
Ba-X	"	"	-	99.5		

Table 4 Self-diffusivities in analcime, chabazite and mordenite ($D^* = D_o \exp -E/RT$)

Zeolite	Composition	$D_o/m^2 s^{-1}$	$E/kJ\ mol^{-1}$	Surface area used and comments	Reference
Na-analcime	Al:Si ~ 1:2	$2.3_5 \times 10^{-9}$	48.1	A; 0.23 - 49.9°C	25
K-analcime (leucite)	"	$2.5_7 \times 10^{-9}$	68.6	A; 25 - 88°C	
Rb-analcime	"	$4.0_4 \times 10^{-11}$	84.0	A; 25.4 - 109.9°C	
Cs-analcime (pollucite)	"	$2.0_9 \times 10^{-9}$	108.7	A; 114 - 196°C	
Na-chabazite	$Ca_{0.03}Na_{1.92}[Al_2Si_{4.98}]$	1.24×10^{-3}	52.8	G; ~ 13 - 50°C	27
K-chabazite	$Ca_{0.03}K_{1.92}[Al_2Si_{5.13}]$	$3.5_9 \times 10^{-6}$	28.4	G; ~ 15 - 46°C	
Na-chabazite	$Ca_{0.05}Na_{0.88}[AlSi_{3.37}]$	$3.9_5 \times 10^{-11}$	27.4 ± 0.5	A; 25 - 65°C	26
K-chabazite	$Ca_{0.03}K_{0.91}[AlSi_{3.07}]$	9.4×10^{-11}	29.3 ± 0.6	A; 14.4 - 54.8°C	
Rb-chabazite	$Na_{0.13}Rb_{0.82}[AlSi_{2.34}]$	$1.7_3 \times 10^{-10}$	28.2 ± 0.5	A; 2.6 - 44.8°C	
Cs-chabazite	$Ca_{0.07}Cs_{0.81}[AlSi_{3.16}]$	$1.6_8 \times 10^{-11}$	31.6 ± 0.6	A; 0.5 - 79.8°C	
Ca-chabazite	$Ca_{0.44}Na_{0.08}[AlSi_{2.94}]$	$5.5_1 \times 10^{-10}$	57.7 ± 1.7	A; 25.1 - 74.8°C	
Sr-chabazite	$Na_{0.08}Sr_{0.44}[AlSi_{2.77}]$	$1.0_1 \times 10^{-9}$	61.0 ± 1.8	A; 25.9 - 77.3°C	
Ba-chabazite	$Na_{0.08}Ba_{0.44}[AlSi_{3.03}]$	$3.9_7 \times 10^{-11}$	36.9 ± 1.1	A; 30.0 - 75.4°C	
Na-mordenite	$K_{0.01}Na_{0.97}[AlSi_{5.26}]$	$4.8_9 \times 10^{-11}$	36.5	A; 10 -.55°C	33
K-mordenite	$K_{0.96}Na_{0.04}[AlSi_{5.26}]$	$2.1_1 \times 10^{-12}$	29.8	A; 41.5 - 67.5°C	
Rb-mordenite	$K_{0.96}Na_{0.04}[AlSi_{5.26}]$	$8.5_1 \times 10^{-1}$	84.7	A; 22 - 41.5°C	
Cs-mordenite	$Na_{0.02}Cs_{0.98}[AlSi_{5.26}]$	$9.7_2 \times 10^{-12}$	18.0	A; 28.7 - 97.2°C	
Ca-mordenite	$Ca_{0.36}K_{0.01}[AlSi_{5.36}]$	$3.6_5 \times 10^{-14}$	43.7	A; 27 - 93°C	
Sr-mordenite	$K_{0.02}Na_{0.49}Sr_{0.25}[AlSi_{5.30}]$	$3.8_6 \times 10^{-9}$	66.8	A; 29.5 - 75°C	
Ba-mordenite	$Ba_{0.37}K_{0.01}Na_{0.26}[AlSi_{5.40}]$	$9.7_2 \times 10^{-9}$	42.4	A; 18.5 - 77.5°C	

Ion valence as well as ion size influences the size of the hydration shell.

(v) The substantial values of E for ionic conductivity in anhydrous zeolite X, [39] despite its very open structure, indicates large changes in electrical potential over distances less than that of a unit ion migration step. These changes are illustrated by calculations of electrical potential inside heulandite [41] and by calculations of electrostatic fields in zeolites A and X [42,43].

For self-diffusion of Na^+ in zeolites A and X [28,29,30] and of Zn^{2+} in A [31] the exchange kinetics have been interpreted in terms of two simultaneous processes. Hoinkis and Levi [30] considered that two independent processes occurred in X, respectively via the channel system of 26-hedra and the channel system of sodalite cages and hexagonal prisms. It is however difficult to see why these processes should not be coupled, and it has instead been proposed that diffusion is linked with a slow reversible ion localisation-delocalisation process [28,29]. Table 2 records the result of each method of analysis, in the latter instance according to the relation

$$\partial C_1/\partial t = (D^*/r^2)\partial/\partial r(r^2 \partial C_1/\partial r) + k_2(C_2 - \alpha_{12} C_1) \qquad (33)$$

C_1 is the concentration of traced mobile ions (in the 26-hedra); C_2 is that of localised traced ions (e.g. in sodalite cages or (for Na-X) in hexagonal prisms); r is the crystal radius (treating crystals as spheres all of one size); k_2 is the rate constant for delocalisation; and $\alpha_{12} = C_2/C_1$. It has the value 2 for Na-A, with its 8 "bound" and 4 "mobile" Na^+ per unit cell. Table 2 records this analysis in terms of $D^* = D_o \exp -E/RT$ and $k_2 = k_o \exp -E_1/RT$.

The results in Tables 2 to 4 refer to zeolites of fixed composition, usually nearly homoionic. However D* for a given cation may depend on the cationic composition of the zeolite. This aspect has been studied in (K,Na)-mordenite [33] and -chabazite [27]. For chabazite D^*_{Na} and D^*_K both varied monotonically with composition but in mordenite these diffusivities appeared to vary in a more complex way. The self-diffusivities are related to the phenomenological coefficients of the irreversible thermodynamic formulation of cation diffusion but so far there is no treatment of the concentration dependence of these coefficients.

CONCLUDING REMARK

In this account I have not tried to cover the extensive experimental material in the literature because any brief account would then necessarily be shallow. Instead certain basic topics have been considered in more depth to show the stage of development, and in the hope of stimulating further work.

REFERENCES

1. R.M. Barrer in "Natural Zeolites, Occurrence, Properties, Use" Editors L.B. Sand and F.A. Mumpton (Pergamon) 1978, p.385.
2. R.M. Barrer and J.D. Falconer, Proc. Roy. Soc., 1956, A 236, 227.
3. R.M. Barrer and B.M. Munday, J. Chem. Soc. A, 1971, 2909.
4. R.M. Barrer and B.M. Munday, J. Chem. Soc. A, 1971, 2914.
5. R.M. Barrer and L. Hinds, J. Chem. Soc., 1953, 1879.
6. H.B. Callen, S.E. Harrison and C.J. Kriessman, Phys. Rev., 1956, 103, 851.

7. C. Borghese, J. Phys. Chem. Solids, 1967, 28, 2225.
8. R.F. Mueller, J. Phys. Chem. Solids, 1967, 28, 2239.
9. J.E. Grover and P.M. Orville, Geochim. et Cosmochim. Acta, 1969, 33, 205.
10. R.F. Mueller, S. Ghose and S.K. Saxena, Geochim. et Cosmochim. Acta, 1970, 34, 1356.
11. W.J. Walker and K. Rodgers, Geochim. et Cosmochim. Acta, 1974, 38, 1521.
12. J. Grover, Geochim. et Cosmochim. Acta, 1974, 38, 1527.
13. G.L. Gaines and H.C. Thomas, J. Chem. Phys., 1953, 21, 714.
14. R.M. Barrer and J. Klinowski, J. Chem. Soc. Faraday I, 1974, 70, 2080.
15. R.M. Barrer and J. Klinowski, J. Chem. Soc. Faraday I, 1979, 75, 247.
16. R.M. Barrer and J. Klinowski, J. Chem. Soc. Faraday I, 1972, 68, 73. Also ref. 19.
17. E. Tambuyzer and H.J. Bosmans, Acta Cryst., 1976, B32, 1714; and C. Baerlocher and R.M. Barrer, Z. Krist., 1974, 140, 10.
18. L.G. Medaris, Amer. J. Sci., 1969, 267, 945.
19. R.M. Barrer and J. Klinowski, Phil. Trans., 1977, 285, 638.
20. R.M. Barrer and J. Klinowski, Geochim. et Cosmochim. Acta, 1979, 43, 755.
21. J. Hijmans and J. de Boer, Physica, 1955, 21, 471.
22. C. Domb, Adv. Phys., 1960, 9, 149.
23. R.M. Barrer and R.P. Townsend, J. Chem. Soc. Faraday I, 1976, 72, 661.
24. W. Loewenstein, Amer. Mineralog., 1954, 39, 92.
25. R.M. Barrer and L.V.C. Rees, Trans. Faraday Soc., 1960, 56, 709.
26. R.M. Barrer, R.F. Bartholomew and L.V.C. Rees, J. Phys. Chem. Solids, 1963, 24, 51.
27. S.C. Duffy and L.V.C. Rees, J. Chem. Soc. Faraday I, 1974, 70, 777.
28. L.M. Brown, H.S. Sherry and F.J. Krambeck, J. Phys. Chem., 1971, 75, 3846.
29. L.M. Brown and H.S. Sherry, J. Phys. Chem., 1971, 75, 3855.
30. E. Hoinkis and H.W. Levi, Z. Naturforsch., 1968, A24, 813.
31. V.M. Radak, I.J. Gial and J.S. Salai, J. Chem. Soc. Faraday I, 1976, 72, 1150.
32. A. Dyer and J.M. Fawcett, J. Inorg. Nucl. Chem., 1966, 28, 615.
33. L.V.C. Rees and A. Rao, Trans. Faraday Soc., 1966, 62, 2103.
34. A. Dyer, R.B. Gettins and R.P. Townsend, J. Inorg. Nucl. Chem., 1970, 32, 2395.
35. A. Dyer and R.B. Gettins, J. Inorg. Nucl. Chem., 1970, 32, 2401.
36. E. Hoinkis and H.W. Levi, Soc. Chem. Ind., Conference on Ion Exchange in the Process Industries, London, 1969.
37. A. Dyer and A.B. Ogden, J. Inorg. and Nucl. Chem., 1975, 37, 2207.
38. A. Dyer and A.B. Ogden, J. Chromat., 1974, 102, 95.
39. D.C. Freeman and D.N. Stamires, J. Chem. Phys., 1961, 35, 799.
40. R.M. Barrer and H.T. Chio, J. Polymer Sci., Part C, 1965, No.10, 111.
41. D. Bonnin and A.P. Legrand, Chem. Phys. Letters, 1975, 30, 296.
42. E. Dempsey in "Molecular Sieves", Soc. Chem. Ind., London, 1968, p.293.
43. R.M. Barrer and R.M. Gibbons, Trans. Faraday Soc., 1963, 59, 2569; and 1965, 61, 948.